



HAL
open science

**Mycobacterium smegmatis
phosphoinositols-glyceroarabinomannans. Structure and
localization of alkali-labile and alkali-stable
phosphoinositides.**

M. Gilleron, N. Himoudi, O. Adam, P. Constant, A. Venisse, M. Rivière, G.
Puzo

► **To cite this version:**

M. Gilleron, N. Himoudi, O. Adam, P. Constant, A. Venisse, et al.. Mycobacterium smegmatis phosphoinositols-glyceroarabinomannans. Structure and localization of alkali-labile and alkali-stable phosphoinositides.. Journal of Biological Chemistry, 1997, 272 (1), pp.117-24. 10.1074/jbc.m109.037846 . hal-00177659

HAL Id: hal-00177659

<https://hal.science/hal-00177659>

Submitted on 22 Mar 2021

HAL is a multi-disciplinary open access archive for the deposit and dissemination of scientific research documents, whether they are published or not. The documents may come from teaching and research institutions in France or abroad, or from public or private research centers.

L'archive ouverte pluridisciplinaire **HAL**, est destinée au dépôt et à la diffusion de documents scientifiques de niveau recherche, publiés ou non, émanant des établissements d'enseignement et de recherche français ou étrangers, des laboratoires publics ou privés.

Mycobacterium smegmatis Phosphoinositols-Glyceroarabinomannans

STRUCTURE AND LOCALIZATION OF ALKALI-LABILE AND ALKALI-STABLE PHOSPHOINOSITIDES*

(Received for publication, April 22, 1996, and in revised form, October 16, 1996)

Martine Gilleron, Nourédine Himoudi, Olivier Adam, Patricia Constant, Anne Venisse, Michel Rivière, and Germain Puzo‡

From the Institut de Pharmacologie et de Biologie Structurale du Centre National de la Recherche Scientifique, 118 route de Narbonne, 31062 Toulouse Cedex, France

Lipoarabinomannans from fast growing *Mycobacterium sp.*, namely AraLAMs, stimulate the early events of macrophage activation. The immunological activities of all of these AraLAMs drastically decrease with the loss of the mild alkali groups, which were believed to be restricted to the fatty acid residues from the phosphatidyl-*myo*-inositol anchor. This report reveals the presence and the structure of mild alkali-labile phosphoinositide units linked via the phosphate to the C-5 of the β -D-Araf in the AraLAMs of *Mycobacterium smegmatis*, a fast growing mycobacterial species. Their structure was unambiguously established with a strategy based on both one-dimensional ^{31}P and two-dimensional ^1H - ^{31}P heteronuclear multiple quantum correlation spectroscopy (HMQC) and HMQC-homonuclear Hartmann-Hahn spectroscopy NMR experiments applied to native AraLAMs and to AraLAMs treated in mild alkali conditions. Next to these alkali-labile phosphoinositides estimated at three per molecule, two other mild alkali-stable phosphoinositide units were identified: the expected (*myo*-inositol-1)-phosphate-(3-glycerol) unit typifying the well known glycosylphosphatidylinositol anchor of the mannan core and, more surprisingly, one (*myo*-inositol-1)-phosphate-(5- β -D-Araf) unit having the same structure as the alkali-labile ones. Moreover, these four phosphoinositide units were found capping the arabinan side chains. Thus, their different behavior toward mild alkaline hydrolysis was explained according to their accessibility to the alkali reagent. This novel class of LAMs, namely phosphoinositols-glyceroarabinomannans (PI-GAMs), are characterized by their phosphoinositide units but also by the absence of fatty acid residues. These PI-GAMs were found to elicit the secretion of tumor necrosis factor- α , suggesting that phosphoinositides are the major PI-GAM epitope involved in this process.

In recent years, the immunological findings concerning lipoarabinomannans (LAMs)¹ have indicated that they play a

* This work was supported by grants from the Région Midi Pyrénées (RECH/9307911). The costs of publication of this article were defrayed in part by the payment of page charges. This article must therefore be hereby marked "advertisement" in accordance with 18 U.S.C. Section 1734 solely to indicate this fact.

‡ To whom correspondence and reprint requests should be addressed. Tel.: 33-0561335912; Fax: 33-0561335886.

¹ The abbreviations used are: LAM, lipoarabinomannan; AraLAM, LAM without mannosyl extensions; dAraLAM, deacylated AraLAM; BCG, bacillus Calmette Guérin; DEPT, distortionless enhancement by polarization transfer; dLAM, deacylated LAM; GC/MS, gas chromatography/mass spectrometry; HMQC, heteronuclear multiple quantum

key role in tuberculosis immunopathogenesis (1). These lipopolysaccharide-like molecules are ubiquitously found in the cell walls of the *Mycobacterium* genus (2). According to their structure, LAMs have been classified into two types, the mannosylated LAMs, called ManLAMs, and the AraLAMs. ManLAMs are characterized by the presence of small α (1–2)-manno-oligosaccharides located at the arabinan side-chain termini. More recently, the ManLAMs have been subdivided into two types according to the presence or absence of phosphatidyl-*myo*-Ins anchor (3). ManLAMs were first isolated from the *Mycobacterium tuberculosis* Erdman strain (4, 5) and further from the vaccine strain *Mycobacterium bovis* BCG (6, 7). AraLAMs are devoid of manno-oligosaccharide caps, but the presence of *myo*-Ins phosphate units capping a minor portion of the AraLAM arabinan side chains was recently established (8). These AraLAMs arise from an unidentified fast growing mycobacterial strain that was initially considered as H37Ra (9).

AraLAMs mediate the early activation of macrophages. They stimulate early gene responses, at the mRNA level, of the *c-fos* gene and chemotactic JE and KC cytokines (10, 11), but they also induce transcription of the mRNA for cytokines characteristically produced by macrophages (tumor necrosis factor- α and interleukins 1- α , 1- β , 6, 8, and 10). The TNF- α transcription induced by AraLAMs was blocked by monoclonal antibodies against CD14, an LPS receptor (12).

These AraLAM activities dramatically decrease when ManLAMs are used (10), in agreement with the fact that virulent organisms survive and multiply within the infected macrophages. However, ManLAMs mediate other major specific interactions between immune cells and mycobacteria. It was demonstrated that the ManLAMs from *M. tuberculosis* and *M. bovis* BCG bind selectively to murine and human macrophages through the mannose receptor (13, 14), suggesting that they mediate the binding of these mycobacteria to the alveolar macrophages. More recent data (15) indicate that double negative human CD4⁺ CD8⁺ $\alpha\beta$ T-cell lines recognize ManLAMs from *M. tuberculosis* and *Mycobacterium leprae* presented by human CD1b molecules.

All these ManLAM and AraLAM properties disappear after mild alkaline treatment, revealing the key role of the alkali-labile residues (16, 17). To date, from the ManLAM and AraLAM structural models proposed, these alkali residues are restricted to the fatty acids of the *myo*-Ins phosphatidyl anchor.

correlation spectroscopy; HOHAHA, homonuclear Hartmann-Hahn spectroscopy; $^3J_{\text{H,H}}$, vicinal spin-spin coupling constants; ManLAM, LAM with mannosyl extensions; P1 and P2, phosphates 1 and 2, respectively; PI-GAM, phosphoinositol-glyceroarabinomannan; TMS, trimethylsilylation; TNF, tumor necrosis factor; Ins, inositol; Gro, glycerol; t-, terminal; LPS, lipopolysaccharide; SW, spectral width; TPPI, time-proportional phase increment.

However, Hunter and Brennan (18) reported the existence of alkali-stable and alkali-labile *myo*-Ins in the LAMs from H37Ra. The alkali-stable *myo*-Ins was assigned to the phosphatidyl-*myo*-Ins anchor located at the nonreducing end of the mannan core. Its structure was completely elucidated by two-dimensional NMR ^1H - ^{31}P heteronuclear multiple quantum correlation spectroscopy-homonuclear Hartmann-Hahn (HMQC-HOHAHA) experiments, unambiguously establishing that the anchor was part of the LAMs and not due to possible phosphatidylinositol mannoside contamination (3). However, the precise location of the alkali-labile *myo*-Ins phosphate residues as well as their substituent structures were unknown (18).

Mycobacterium smegmatis is a fast growing mycobacterial strain. A serologically active acidic arabinomannan was purified from *M. smegmatis* by Weber and Gray (19) and was fractionated into phosphorylated and nonphosphorylated molecules. Preliminary structural studies revealed that both forms have similar core structures characterized by 1→5-linked *Araf* residues attached to O-4 of *Arap* and 6-O-linked α -D-*Manp* residues. In the present work, we have undertaken to explore the structure of the LAMs from *M. smegmatis* obtained by solvent cell wall extraction, using NMR spectroscopy, and more particularly, we address the question of the existence of alkali-stable and alkali-labile *myo*-Ins phosphates, their substituent structures, and their locations.

EXPERIMENTAL PROCEDURES

Extraction and Purification of AraLAMs, Deacylation, and Subsequent Purifications—The extraction and purification of *M. smegmatis* ATCC 607 AraLAMs were performed as described previously for the ManLAMs from *M. bovis* BCG (6). The *M. smegmatis* native LAMs monitored by SDS-polyacrylamide gel electrophoresis show a broad band located around 30 kDa, indicating that LAMs were not contaminated by lipomannans.

dAraLAMs were prepared from the crude fraction containing lipoglycan, namely LAMs and lipomannans (60 mg) treated with 0.1 N NaOH for 2 h at 40 °C followed by gel filtration on a Bio-Gel G75 column eluted by 0.1 N CH_3COOH . The dLAM fractions were characterized by GC after hydrolysis and derivatization by a molar ratio of Ara to Man of 1.45:1.

Native AraLAMs (10 mg) were submitted to mild alkaline hydrolysis (0.1 N NaOD at 40 °C) in an NMR tube, and the reaction was monitored at different times (30 min, 1 h, 1 h 30 min, and 2 h) by ^{31}P one-dimensional NMR spectroscopy. Then partial acidic hydrolysis of the dAraLAMs was performed with 0.06 N HCl for 15 min at 100 °C, and the hydrolysate after cooling was applied on a Bio-Gel P-4 column eluted by water. The collected samples were characterized by gas-liquid chromatography after hydrolysis (2 N trifluoroacetic acid for 2 h at 100 °C) and TMS derivatization.

Native AraLAMs (5 mg) were submitted in a NMR tube to partial acidic hydrolysis (0.1 N DCl for 15 min at 80 °C). The reaction was monitored by one-dimensional ^{31}P NMR. The products of the reaction were then submitted to mild alkaline hydrolysis (0.1 N NaOD for 1 h at 40 °C) with no intermediate purification.

AraLAMs were O-methylated three times according to a modified (6) procedure of Ciucanu and Kerek (20). Per-O-methylated LAMs were hydrolyzed with 2 N trifluoroacetic acid at 120 °C for 2 h, reduced with NaBD_4 , and acetylated. The alditol acetates were identified by GC/MS and quantified by GC. Table I reveals the presence per LAM molecule of the same ratio of t-*Araf* units and 3,5-di-O-linked *Araf* units.

Routine gas chromatography was performed on a Girdel series 30 chromatograph equipped with an OV1 wall-coated open tubular capillary column (25-m length \times 0.22-mm inner diameter; Spiral, Dijon, France) using helium gas at a flow rate of 2.5 ml/min with a flame ionization detector at 310 °C. A temperature program from 100 to 280 °C at a speed of 3 °C/min was used. The injector temperature was 260 °C for TMS glycoside analysis. GC/MS analysis was performed on a Hewlett-Packard 5889X mass spectrometer (electron energy, 70 eV) working in both electron impact and chemical ionization modes, coupled with a Hewlett-Packard 5890 gas chromatograph series II fitted with an OV1 column (12 m \times 0.30 mm).

NMR spectra were recorded on a Bruker AMX-500 spectrometer equipped with an Aspect X32 computer. Samples were exchanged in D_2O (Spin et Techniques, Paris, France; 99.9% purity) with intermedi-

TABLE I
Methylation analysis of AraLAMs from *M. smegmatis*

Full name of the partially methylated alditol acetate derivative	Abbreviated name of the glycosyl residue	LAM ^a mol%
2,3,5-Tri-O-Me-1,4-di-O-Ac-arabinitol	t- <i>Araf</i>	11
3,5-Di-O-Me-1,2,4-tri-O-Ac-arabinitol	2-O-Linked <i>Araf</i>	9
2,3-Di-O-Me-1,4,5-tri-O-Ac-arabinitol	5-O-Linked <i>Araf</i>	45
2-O-Me-1,3,4,5-tetra-O-Ac-arabinitol	3,5-Di-O-linked <i>Araf</i>	11
2,3,4,6-Tetra-O-Me-1,5-di-O-Ac-mannitol	t- <i>Manp</i>	12
2,3,4-Tri-O-Me-1,5,6-tri-O-Ac-mannitol	6-O-Linked <i>Manp</i>	5
3,4-Di-O-Me-1,2,5,6-tetra-O-Ac-mannitol	2,6-Di-O-linked <i>Manp</i>	7

^a Average values from three experiments.

ate lyophilization and then dissolved in 99.96 atom % D_2O at a concentration of 40 mg/ml for the native LAMs and 6 mg/ml for the dLAMs and analyzed in a 200 \times 5-mm 535-PP NMR tubes. ^1H Chemical shifts are expressed in ppm downfield from the signal for internal 3-(trimethylsilyl)-propane sulfonic acid sodium salt ($\delta_{\text{H/TMS}}$ 0.015).

The one-dimensional proton (^1H) spectrum was measured using a 30–90° tipping angle for the pulse and 1 s as a recycle delay between each of the 256 acquisitions of 1.64 s. The spectral width of 5005 Hz was collected in 16,000 complex points that were multiplied by an exponential function (LB = 2 Hz) prior to processing to 32,000 real points in the frequency domain. After Fourier transformation, the spectra were base line-corrected with a fourth order polynomial function.

The one-dimensional phosphorus (^{31}P) spectra were measured at 202 MHz by employing a spectral width of 25 kHz, and phosphoric acid (85%) was used as the external standard (δ_{P} 0.0). The data were collected in 32,000 complex data sets, and an exponential transformation (LB = 5 Hz) was applied prior to processing to 64,000 real points in the frequency domain.

All two-dimensional NMR data sets were recorded at 35 °C without sample spinning, and data were acquired in the phase-sensitive mode using the time-proportional phase increment (TPPI) method (21).

The two-dimensional HOHAHA spectrum was recorded using a MLEV-17 mixing sequence of 30 ms (22). The spin-lock field strength corresponded to a 90° pulse width of 30 μs . The spectral width was 5000 Hz in each dimension. The HOD signal was presaturated for 1 s during the relaxation delay. 1024 spectra of 4096 data points with 16 scans/ t_1 increment were recorded.

^1H - ^{31}P and ^1H - ^{13}C correlation spectra were recorded in the proton-detected mode with a Bruker 5-mm ^1H broad band tunable probe with reversal geometry. The single-bond correlation spectra (HMQC) of ^1H - ^{13}C and ^1H - ^{31}P were obtained according Bax's pulse sequence (23). The GARP sequence (24) at the carbon or phosphorus frequency was used as a composite pulse decoupling during acquisition. For the ^1H - ^{13}C HMQC spectrum, spectral widths of 16,250 Hz in ^{13}C and 4500 Hz in ^1H dimensions were used to collect a 4096 \times 400 (TPPI) point data matrix with 32 scans/ t_1 value expanded to 4096 \times 1024 by zero filling. The relaxation delay was 1.2 s. A sine bell window shifted by $\pi/2$ was applied in both dimensions. The ^1H - ^{31}P HMQC spectrum was obtained with a 4096 \times 80 (TPPI) point data matrix with 64 scans/ t_1 value. The spectral window was 4003 Hz in F2 dimension (^1H) and 810 Hz in F1 dimension (^{31}P). Relaxation delay was 1.2 s. The original data matrix point was expanded to a 4096 \times 512 real matrix. The pulse sequence used for ^1H -detected heteronuclear relayed spectra (HMQC-HOHAHA) ^1H - ^{31}P was that of Lerner and Bax (25). These spectra were obtained with a 4096 \times 80 (TPPI) point data matrix with 64 scans/ t_1 value. The spectral window was 4003 Hz in F2 dimension (^1H) and 810 Hz in F1 dimension (^{31}P). The relaxation delay was 1.2 s, and different experiments were realized with different mixing times. The original data matrix was expanded to a 4096 \times 512 real matrix.

TNF- α Assay—THP-1 monocyte/macrophage human cell line was maintained as nonadherent cells in continuous culture with Iscove's modified Dulbecco's medium (Life Technologies, Inc.), 10% fetal calf serum (Life Technologies) in an atmosphere of 5% CO_2 at 37 °C. The purified molecules were added in duplicate to THP-1 cells (0.5×10^6 cells/well) in 24-well tissue culture plates and then incubated for 6 h at 37 °C. Stimuli were previously incubated 1 h at 37 °C in the presence or absence of 10 $\mu\text{g}/\text{ml}$ polymyxin B (Sigma) known to inhibit the effect of LPS (26). Culture supernatants were then assayed for TNF using the previously described cytotoxic assay against WEHI164 clone 13 cells (27). Each supernatant was tested at two dilutions (1:2 and 1:20) in duplicate. The assay was performed as follows. 50 μl of sample were added to 50 μl of WEHI cells (4×10^5 cells/ml) in flat-bottom 96-well

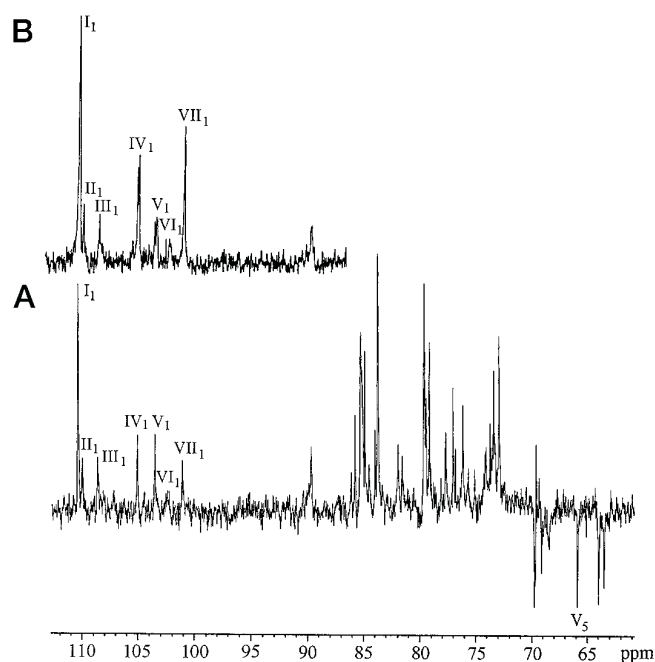


FIG. 1. A, J -modulated ^{13}C one-dimensional spectrum of the dLAMs from *M. smegmatis*. B, expanded zone ($\delta^{13}\text{C}$ 87.5–113.0) of the DEPT ^{13}C one-dimensional spectrum of the dLAMs from *M. bovis* BCG. Glycosyl residues are labeled in *roman numerals*, and their carbons are labeled in *arabic numerals*. I, 5-*O*-linked α -Araf; II, 3,5-di-*O*-linked α -Araf; III, 2-*O*-linked α -Araf; IV, t- α -Manp; V, t- β -Araf; VI, 6-*O*-linked α -Manp; VII, 2-*O*-linked and 2,6-di-*O*-linked α -Manp.

plates. In each experiment, a reference curve was obtained using serial dilutions of human recombinant TNF- α (Life Technologies) starting at 5000 down to 1 pg/ml. After a 20-h incubation at 37 °C, 50 μl of tetrazolium salts (1 mg/ml 3-(4,5-dimethyl thiazol-2-yl)-2,5-diphenyl tetrazolium bromide in Iscove's modified Dulbecco's medium, Sigma) were added to each well and incubated for 4 h. Formazan crystals were solubilized with 100 μl of lysis buffer (*N,N*-dimethyl formamide, 30% SDS (1:2) adjusted at pH 4.7 with acetic acid), and optical density was read at 570 nm with an enzyme-linked immunosorbent assay plate reader.

RESULTS

Determination of the *M. smegmatis* LAM Class—Fig. 1A presents the J -modulated ^{13}C one-dimensional spectrum of the LAMs from *M. smegmatis* treated in mild alkaline conditions called dLAMs. This spectrum shows the same anomeric carbon resonances as those present in the partial DEPT ^{13}C one-dimensional spectrum of the *M. bovis* BCG dLAMs (Fig. 1B). However, they differ by their relative intensity in the anomeric as well as in the exocyclic aliphatic carbon regions (not shown). First, the resonances at 103.42 ppm (V_1) and 65.77 ppm (V_5) (Fig. 1A), assigned to the C-1 and C-5 of t- β -Arafs, are relatively more intense than those of the analogous carbons of the *M. bovis* BCG dLAMs, so the *M. smegmatis* LAMs contain relatively more t- β -Araf units than the *M. bovis* BCG ones. The second major difference is the decrease of the anomeric carbon resonance intensity at δ 101.01 (VII_1) (Fig. 1A) assigned to 2,6-di-*O*-linked α -Manps and maybe to 2-*O*-linked α -Manps, the latter of which are the ManLAM reporter units. In order to clarify this assignment, the *M. smegmatis* dLAM ^1H - ^{13}C HMQC spectrum was recorded (Fig. 2). The C-1 resonance at δ 101.01 (VII_1) correlated with one anomeric proton signal at 5.12 ppm, while in the *M. bovis* BCG dManLAM HMQC spectrum (6), this C-1 resonance correlated with two H-1 signals at 5.25 and 5.22 ppm. These protons were assigned to the H-1s of 2,6-di-*O*-linked α -Manps and 2-*O*-linked Manps corresponding, respectively, to the Manps from the mannan core and from the manno-oligosaccharide caps. So these data unambiguously re-

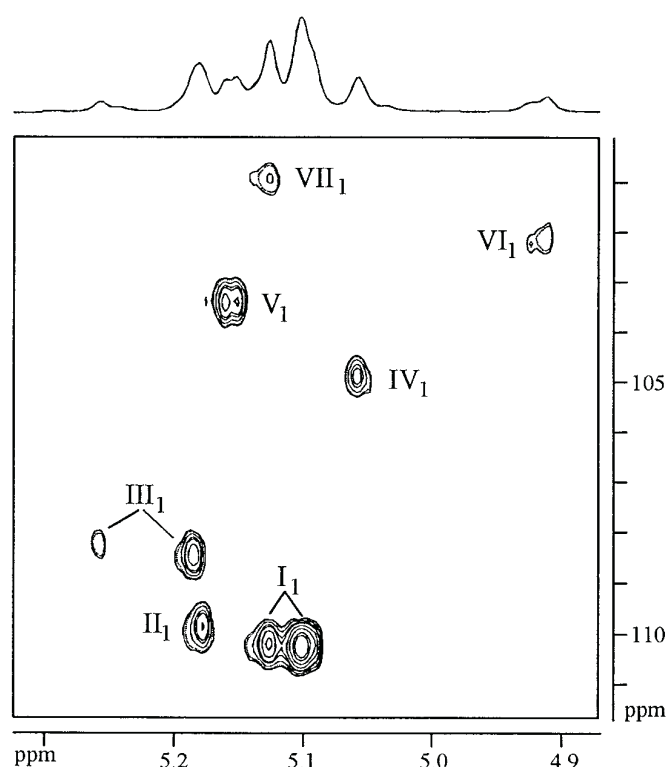


FIG. 2. Expanded region ($\delta^1\text{H}$ 4.85–5.33; $\delta^{13}\text{C}$ 100.0–111.5) of the ^1H - ^{13}C HMQC spectrum of *M. smegmatis* dLAMs. Glycosyl residues are labeled in *roman numerals*, and their carbons are labeled in *arabic numerals*. I, 5-*O*-linked α -Araf; II, 3,5-di-*O*-linked α -Araf; III, 2-*O*-linked α -Araf; IV, t- α -Manp; V, t- β -Araf; VI, 6-*O*-linked α -Manp; VII, 2,6-di-*O*-linked α -Manp.

veal the absence of 2-*O*-linked Manp units in the LAMs of *M. smegmatis*. Likewise, a single correlation was observed between the *M. smegmatis* dLAM t- β -Araf C-1 resonance at 104.93 ppm (IV_1) and the anomeric proton at 5.06 ppm. In the case of the *M. bovis* BCG LAMs, this anomeric carbon correlated with two H-1 signals assigned to the t- β -Arafs from the mannan core and the manno-oligosaccharide caps. So, this result demonstrates that *M. smegmatis* LAMs contain a single type of t- β -Arafs restricted to the mannan core. Thanks to the ^1H - ^{13}C HMQC comparative analysis, we propose that the *M. smegmatis* LAMs are devoid of α -Manp-(1 \rightarrow 2)- α -Manp(1 \rightarrow) $_n$ ($0 < n < 2$) oligosaccharides capping the arabinan side chains and thus belong to the AraLAM class.

AraLAM Phosphorylation State—The native AraLAMs were analyzed by one-dimensional ^{31}P NMR spectroscopy (Fig. 3). The one-dimensional ^{31}P spectrum shows two distinct resonances at -0.11 ppm (P1) and -0.35 ppm (P2) with an integration ratio P2:P1 of 4. The P2 and P1 chemical shifts, which are not significantly affected by shifting the pD value from 6 to 10, were assigned to phosphodiester groups (28). The P1 resonance was tentatively assigned to the anchor phosphate based on the phosphate chemical shift (-0.1 ppm) of the phosphatidyl-*myo*-Ins anchor of *M. bovis* BCG ManLAMs (3). Moreover, from a previous study the mild alkali-stability of this phosphodiester linkage was established (3). Then, in order to support the P1 assignment, the AraLAMs were submitted to mild alkaline hydrolysis (0.1 N NaOD, 40 °C), and the reaction products were monitored by one-dimensional ^{31}P NMR spectroscopy. After 30 min of mild alkaline hydrolysis (Fig. 4B), the P2:P1 ratio value decreases from 4 (Fig. 4A) to approximately 1 and remains constant with longer reaction times: 30 min (Fig. 4B) and 2 h (Fig. 4C). These data highlight the presence of three mild alkali-labile phosphate units (P2) and two mild

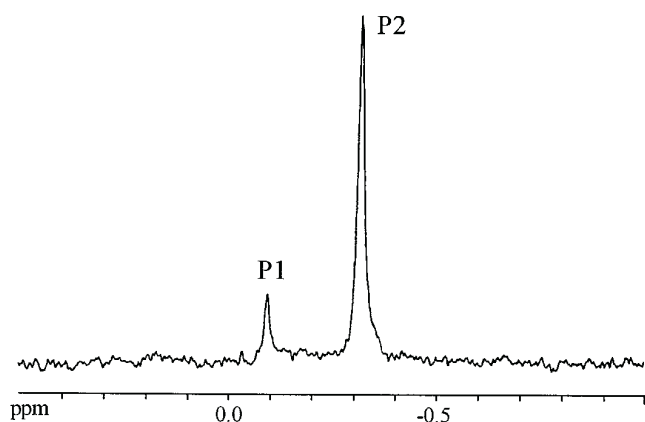


FIG. 3. One-dimensional ^{31}P NMR spectrum ($\delta^{31}\text{P} -1.0$ – 0.5) of the native *M. smegmatis* AraLAMs. The spectrum was recorded in D_2O at pH 7.1 and 308 K (ns 1440, SW 6 ppm).

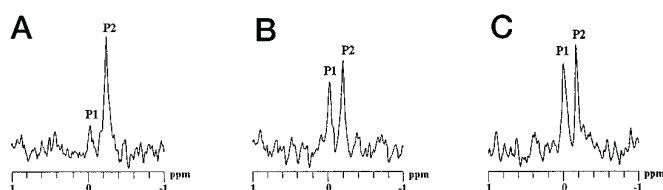


FIG. 4. One-dimensional ^{31}P NMR spectra ($\delta^{31}\text{P} -1.00$ – 1.00) of *M. smegmatis* AraLAMs (A) and after 30 min (B) and 2 h (C) of mild alkali hydrolysis (0.1 N NaOD, 40 °C). The spectra were recorded in D_2O at pH 8.5 and 313 K (ns 100, SW 15 ppm).

alkali-stable phosphates (P1 and P2). One of the alkali-stable phosphate, probably P1, can be assigned to the anchor phosphate, but the presence of a supplementary and unexpected P2 alkali-stable resonance makes this P1 assignment hazardous. So, to demonstrate the P1 attribution and also to establish the substituent structure of the novel P2 alkali-stable unit, the AraLAMs treated in mild alkaline conditions, namely dAraLAMs, were analyzed by two-dimensional ^1H - ^{31}P HMQC (Fig. 5b) and ^1H - ^{31}P HMQC-HOHAHA (Fig. 5c) experiments. The ^1H - ^{31}P HMQC sequence allows the assignment of the protons borne by the carbons involved in the phosphodiester linkage, while the ^1H - ^{31}P HMQC-HOHAHA sequence leads to the definition of the substituent spin systems.

Substituent Structure of the Two Mild Alkali-stable Phosphates, P1 and P2—The dAraLAM ^1H - ^{31}P HMQC spectrum (Fig. 5b) provides correlations between the P1 resonance and three well-defined proton resonances at δ 4.16, δ 4.00, and δ 3.94. Since these protons resonate in an overcrowded area, their assignments based on chemical shifts remain hazardous. To overcome this problem, ^1H - ^{31}P HMQC-HOHAHA spectra were performed with different mixing times. Using a long mixing time (63 ms) (Fig. 5c), the spectrum shows a complex set of correlations. However, the cross-peak at δ 3.39 reveals a well resolved proton resonance correlating on the HOHAHA spectrum (Fig. 5a) with five protons whose chemical shifts and multiplicities agree with a 1-phospho-*myo*-Ins spin system (Table II). In Table II, it can be seen that the *myo*-Ins H-1 (δ 4.16), H-2 (δ 4.35), and H-6 (δ 3.87) are downfield-shifted compared with those of the 1-phospho-*myo*-Ins standard, in agreement with the glycosylation of the *myo*-Ins at the C-6 by the mannan core and at the C-2 by one single α -D-Manp unit. Moreover, the P1 linkage to the *myo*-Ins C-1 was supported by the fact that H-1 (δ 4.16) resonates as a pseudodoublet and as a pseudotriplet in the ^1H - ^{31}P decoupled HMQC-HOHAHA and in the HOHAHA spectra, respectively. The remaining δ 4.00 and δ 3.94 protons from the HMQC spectrum (Fig. 5b) were assigned to the glycerol prochiral H-3 and H-3', while H-1 and H-1' are

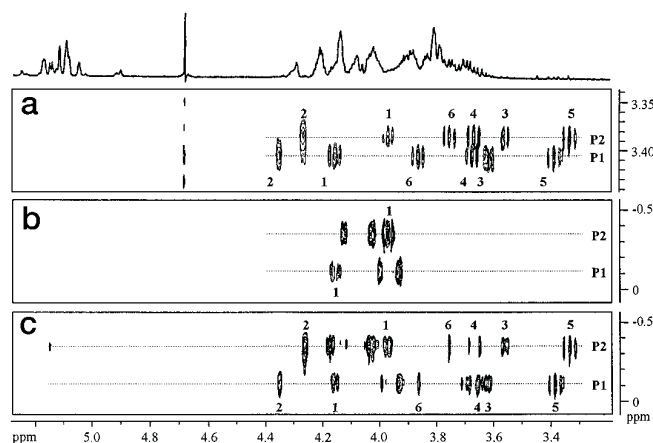


FIG. 5. Partial ^1H - ^1H two-dimensional HOHAHA (a) region ($\delta^1\text{H} 3.20$ – 5.30 and 3.34 – 3.44) spectrum showing the Ins spin systems. Expanded region ($\delta^1\text{H} 3.20$ – 5.30 ; $\delta^{31}\text{P} -0.57$ – 0.08) of the ^{31}P -decoupled, ^1H -detected HMQC (b) and 63-ms HMQC-HOHAHA (c) spectra of dAraLAMs are shown. Numerals correspond to the proton number of the two *myo*-Ins units.

defined from the HMQC-HOHAHA spectrum (Fig. 5c) at 3.70 and 3.73 ppm. The weak intensity cross-peak observed at 3.96 ppm on the HMQC-HOHAHA spectrum, using a short mixing time, reveals a connectivity between P1 and Gro H-2. As expected, it is now clearly established that the alkali-stable P1 corresponds to the phosphate unit of the glycosylphosphatidylinositol anchor.

The same NMR approach was applied in order to determine the substituent structure of the unexpected alkali-stable P2 resonance. As for P1, the HMQC spectrum shows that P2 correlates with three proton resonances at 4.14, 4.04, and 3.99 ppm (Fig. 5b). The HMQC-HOHAHA experiment reveals a complex pattern of connectivities. Again, the proton at 3.34 ppm, which resonates independently in the one-dimensional ^1H spectrum, is attributed to H-5 from a second *myo*-Ins spin system (δ H-1 3.99; δ H-2 4.27; δ H-3 3.57; δ H-4 3.67; δ H-5 3.34; δ H-6 3.77) (Fig. 5a). Likewise, P2 was found to esterify the second *myo*-Ins unit at the C-1 position from the multiplicity of H-1 (t , $J_{1,P} = J_{1,6}$ 9.7 Hz) in the HOHAHA spectrum (Fig. 5a). The H-1, H-2, and H-6 protons are upfield-shifted compared with those of P1 *myo*-Ins resonating at chemical shifts comparable with those of the 1-phospho-*myo*-Ins standard, establishing that positions C-2 and C-6 are not glycosylated (Table II). Therefore, the P2 *myo*-Ins unit is localized at the terminal position. The remaining P2 proton connectivities (δ 4.14, δ 4.04) in the HMQC spectrum (Fig. 5b) can be attributed to geminal protons from an undetermined unit. From the ^1H - ^{31}P HMQC-HOHAHA spectrum (Fig. 5c) a cross-peak with a proton at 5.16 ppm is observed assigned to an anomeric resonance either of 2,6-di-O-linked α -Manp or of t - β -Araf. The $J_{1,2}$ coupling constant value of 3.15 Hz (Fig. 6) typifies a β -Araf unit (expected $J_{1,2}$ of α -Manp and β -Araf of 1.8 and 4.1 Hz (29), respectively). Therefore, the resonances at δ 4.14 and δ 4.04 were attributed to the geminal H-5/H-5' protons of a β -Araf unit, revealing that P2 esterifies this unit at the C-5. This C-5 phosphoester linkage is also supported by the downfield chemical shifts of the H-5/H-5' (δ H-5/H-5' α -L-Araf 3.80/3.68 (30)). In the ^1H - ^{31}P HMQC-HOHAHA spectrum (Fig. 5c), the remaining cross-peak (δ 4.19) is in agreement with the chemical shift of the H-2, H-3, and H-4 α -Araf ring protons (δ H-2 4.04, H-3 3.93, H-4 4.03) (30). Also, the subspectrum at δ -0.35 (Fig. 6) reveals an extra β -Araf ring proton resonance superimposed with the H-5 at 4.04 ppm. Thus, it is proposed that the mild alkali-stable P2 esterifies a terminal *myo*-Ins at the C-1 position and a β -D-Araf at the C-5 position.

TABLE II
myo-Ins proton assignment

Signal	δ		J^a		Multiplicity	δ <i>myo-Ins</i> 1P ^b
	P1	P2	P1	P2		
	<i>ppm</i>		<i>Hz</i>			<i>ppm</i>
H-1	4.16	3.99	$J_{1,2}$ 2.2	2.0	Pseudotriplet	3.90
H-2	4.35 ^c	4.27	$J_{2,3}$ 2.2	2.0	Pseudosinglet	4.23
H-3	3.61	3.57	$J_{3,4}$ 9.2	9.9	Pseudodoublet	3.58
H-4	3.67	3.67	$J_{4,5}$ 9.2	9.4	Triplet	3.64
H-5	3.39	3.34	$J_{5,6}$ 9.6	9.6	Triplet	3.34
H-6	3.87 ^c	3.77	$J_{6,1}$ 9.6	9.7	Triplet	3.74

^a $J_{1,P}$ values of 9.6 (P1) and 9.7 Hz (P2) were measured on the HOHAHA spectrum.

^b Data from Refs. 37 and 38.

^c The substantial downfield shift (0.1 ppm) suggests that these positions are glycosylated.

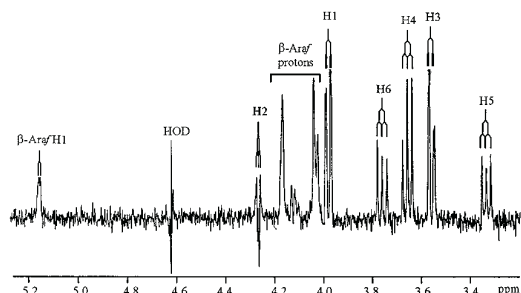


FIG. 6. Subspectrum of the ³¹P-decoupled, ¹H-detected 200 ms HMQC-HOHAHA spectrum of dAraLAMs at $\delta -0.35$. The sweep widths were set to 1841 Hz in F2 dimension and 1012 Hz in F1 dimension. The data matrix point used was 4096×80 with 128 transients for each t_1 increment. The data matrix was zero-filled to 4096×1024 points and multiplied by a $\pi/2$ sine-bell function in both dimensions before Fourier transformation. H1–H6 correspond to the protons of the *myo-Ins* unit.

To support the structure of the (β -Araf-5)-P2-(1-*t-my*o-Ins) motif, the dAraLAMs were hydrolyzed in mild acidic conditions (0.06 N HCl, 15 min, 100 °C). The reaction products were chromatographed on a Bio-Gel P4 eluted with water and monitored for changes in refractive index. The chromatogram (Fig. 7A) shows mainly two peaks. The included sample (*I*) was hydrolyzed (2 N trifluoroacetic acid, 2 h, 100 °C) and was found by GC analysis to be composed almost exclusively of Araf, arising as expected from the arabinan moiety. The void volume (*E*) was subdivided into five fractions (fractions 12–16). By ³¹P one-dimensional NMR analysis, P1 was found in fractions 13 and 14, both P1 and P2 in fraction 15, and P2 alone in fraction 16 (Fig. 7B). This last fraction analyzed by GC after acidic hydrolysis reveals Araf and *myo-Ins*. Moreover, the two-dimensional HOHAHA experiment established that P2 esterifies a terminal *myo-Ins* unit (δ H-1 3.99; δ H-2 4.27; δ H-3 3.57; δ H-4 3.67; δ H-5 3.34; δ H-6 3.77) (not shown). After peracetylation, fast atom bombardment-MS analysis in the negative mode (not shown) demonstrated from the pseudomolecular ions ($M-H$)⁻ at m/z 727 that the major molecular species is Ara-P2-*myo-Ins*. Other pseudomolecular ions are observed in low abundance at m/z 943, 1159, 1375, and 1591, indicating that *myo-Ins*-P2 is also esterified by (Ara)_{*n*} units, where $n = 2-5$, respectively.

Taken together, these data allow us to propose the structure (β -Araf-5)-P2-(1-*t-my*o-Ins) for the mild alkali-stable P2 phosphate and its localization at the nonreducing end of the arabinan side chains.

Substituent Structure of the Three Mild Alkali-labile P2 Phosphates—In order to determine the substituent structures of the alkali-labile P2 phosphates, the native AraLAMs were analyzed by two-dimensional NMR spectroscopy as described previously for the alkali-stable phosphates. As expected from the ratio value of P2:P1 of 4, the P1 cross-peaks in the ¹H-³¹P HMQC-HOHAHA spectrum (Fig. 8) are weaker than those of

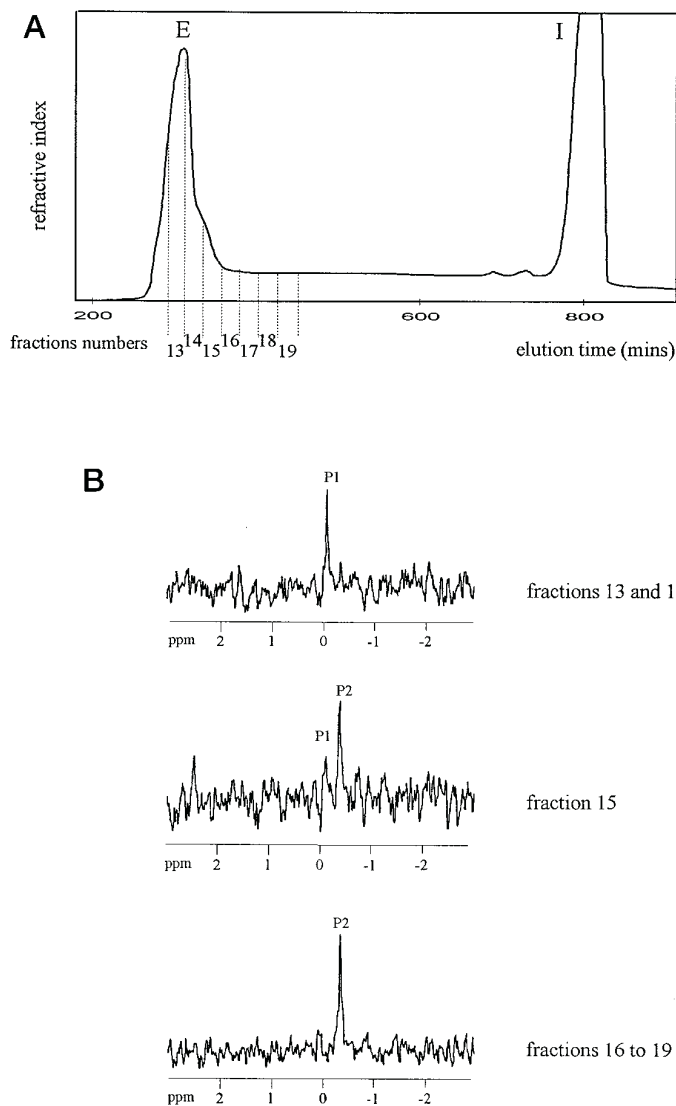


FIG. 7. A, Bio-Gel P-4 chromatography of the dAraLAM hydrolysate (0.06 N HCl, 15 min, 100 °C) eluted with water. The peak corresponding to the void volume (*E*) was collected in different fractions. B, one-dimensional ³¹P NMR spectra (δ ³¹P -3.00 – -3.00) of the indicated void volume fractions. The spectra were recorded in D₂O at pH 8.5 and 308 K.

P2. However, from P1, the *myo-Ins* anchor can be characterized by the proton resonances at δ H1 4.16, δ H2 4.35, δ H3 3.62, δ H4 3.66, δ H5 3.40, and δ H6 3.88, while the glycerol is revealed by the H-3 and H-3' (δ 4.00/3.94) proton resonances. Moreover, from the Gro H-1, H-1', and H-2 chemical shifts (3.70, 3.73, and 3.96 ppm, respectively), it can be advanced that the glycerol is not acylated (31, 32). This assignment was also supported by

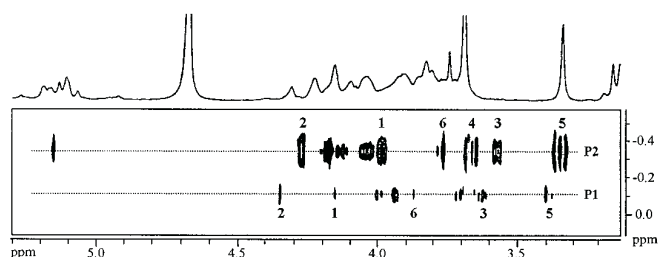


FIG. 8. Expanded region (δ ^1H 3.10–5.30; ^{31}P –0.58–0.10) of the ^{31}P -decoupled, ^1H -detected 63 ms HMQC-HOHAHA spectrum of AraLAMs. Numerals correspond to the proton number of the two *myo*-Ins units.

the absence of C-16 and C-19 methyl fatty ester in routine GC analysis of the hydrolyzed AraLAMs. From P2, this spectrum highlights the same connectivity pattern as for the one observed from P2 resonance of the dAraLAM ^1H - ^{31}P HMQC-HOHAHA spectrum (Fig. 5C), indicating that P2 is linked to β -Araf and to *t-my*o-Ins. The *t-my*o-Ins is characterized by the cross-peaks at δ H1 3.98, δ H2 4.28, δ H3 3.58, δ H4 3.67, δ H5 3.35, δ H6 3.77, while the β -Araf is mainly typified by the P2 connectivity with the H-1 at 5.16 ppm. So, from these data, we propose that the three mild alkali-labile P2 phosphates present the same substituent structures as the mild alkali-stable one, (β -Araf-5)-P2-(1-*t-my*o-Ins). All these phosphoinositide units cap the arabinan side chains, and by analogy to the ManLAMs, these LAMs were called phosphoinositols-glyceroarabinomannans (PI-GAMs), since the phosphatidyl anchor was found to be devoid of C-16 and C-19 fatty acids (see Fig. 10).

To understand the different P2 behavior toward mild alkaline hydrolysis, the following process monitored by ^{31}P one-dimensional NMR spectroscopy was applied to the PI-GAMs *in situ* in the NMR tube. The PI-GAMs were successively hydrolyzed in mild acidic (0.1 N DCl, 80 °C, 15 min) and mild alkaline (0.1 N NaOD, 40 °C, 1 h) conditions. The ^{31}P one-dimensional spectrum (Fig. 9A) of the acidic hydrolysis subproducts is identical to that of the native PI-GAMs (Fig. 3). It is characterized by two phosphodiester resonances P1 and P2 in a ratio approximately of 1:4. P2 arises from the (*Ara*)_{*n*}-P2-*t-my*o-Ins motifs (with *n* = 1–5), while P1 comes from the *my*o-Ins-P-Gro unit of the mannan core. After alkaline hydrolysis, the one-dimensional ^{31}P spectrum (Fig. 9B) is dominated by one phosphodiester resonance assigned to P1. The ratio P2:P1 is approximately 0.2, unambiguously indicating that the P2 alkali-stable unit, observed when the PI-GAMs were treated in mild alkaline conditions, was almost completely hydrolyzed from small oligosaccharides (*Ara*)_{*n*}-P2-*t-my*o-Ins. Thus, it can be advanced that the P2 alkali stability is almost no more observed when the P2 unit is contained by small oligosaccharides. Then it can be proposed that the different behavior toward mild alkaline hydrolysis of the (β -Araf-5)-P2-(1-*t-my*o-Ins) motifs can be explained in terms of PI-GAM conformation (Fig. 10) that prevents the accessibility of the P2 alkali-stable unit to the alkaline reagents.

Induction of TNF- α by Mycobacterial LAM Preparations—The potency of the PI-GAMs to stimulate the production of TNF- α was investigated using the human myelomonocytic cell line THP-1. Monocytes were stimulated by various preparations of LAMs at 10 $\mu\text{g}/\text{ml}$ previously incubated in the presence or absence of polymyxin B (Fig. 11). PI-GAMs, like LPS, induced the THP-1 cells to release TNF- α (250 and 550 $\mu\text{g}/\text{ml}$, respectively). In the presence of polymyxin B, as expected, the LPS was found inactive, while the induction of TNF- α by PI-GAMs was not significantly abrogated. However, the mild alkaline treatment of the PI-GAMs (0.1 N NaOH, 40 °C, 2 h) decreases by a factor of 5 the production of TNF- α . Surpris-

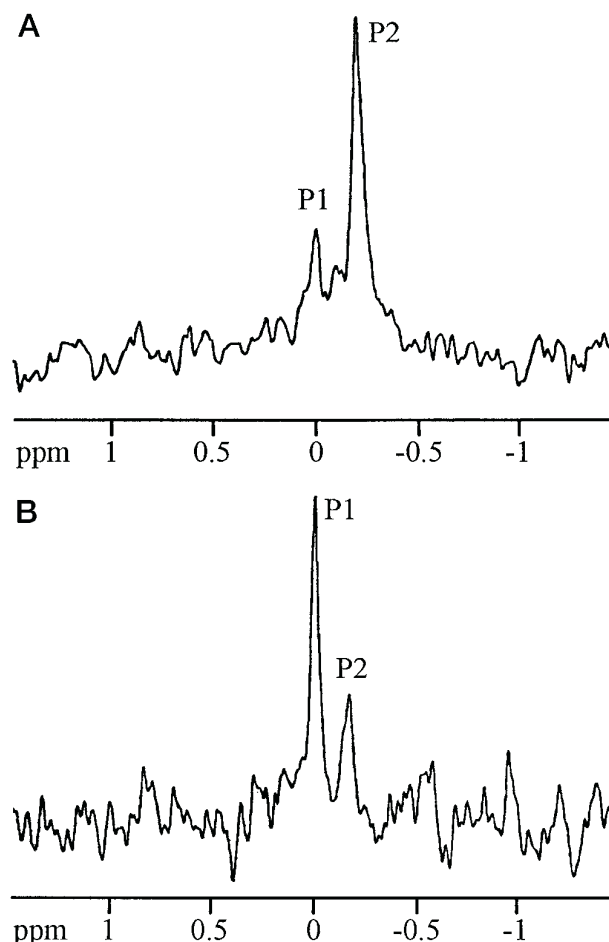


FIG. 9. 1D ^{31}P NMR spectra (δ ^{31}P –1.50–1.50) of *M. smegmatis* AraLAMs. A, after mild acidic hydrolysis (0.1 N DCl, 15 min, 80 °C); the spectrum was recorded in D_2O at pH 7.6 and 313 K (ns 8704, SW 10 ppm). B, after mild alkaline hydrolysis (0.1 N NaOD, 1 h, 40 °C); the spectrum was recorded in D_2O at pH 7.2 and 313 K (ns 1024, SW 10 ppm).

ingly, the *M. smegmatis* LAM fraction devoid of PI-GAMs was inactive in our bioassay even at 50 $\mu\text{g}/\text{ml}$. So, the PI-GAMs appeared to be responsible for the TNF- α induction by the LAM fraction of fast growing mycobacterial species (33).

DISCUSSION

LAMs present a large spectrum of immunological activities involving interactions with B-cells (1), phagocytes (16), and $\alpha\beta$ -T lymphocytes (15). Some molecular targets of LAMs have either been identified as or suggested to be the mannose receptor (13, 14), the CD14 (12) receptor, and more recently the $\alpha\beta$ T-cell receptor (15). In order to define these molecular recognition mechanisms, precise structural models must be proposed for the LAMs. Moreover, in order to determine their role in the immunopathogenesis of mycobacterial diseases, the precise knowledge of the LAM structures according to their mycobacterial origins remains a major objective. Indeed, LAMs that are ubiquitously found in the mycobacterial genus are involved in specific immunological activities according to their mycobacterial source. For example, AraLAMs from a fast growing mycobacterial species present a higher capacity to induce TNF- α than ManLAMs from *M. tuberculosis* strain Erdman (34). Still more relevant is the fact that ManLAMs from *M. leprae* and *M. tuberculosis* activate specifically different $\alpha\beta$ human T-cell lines CD4^- and CD8^- (15).

From a structural point of view, whatever their mycobacte-

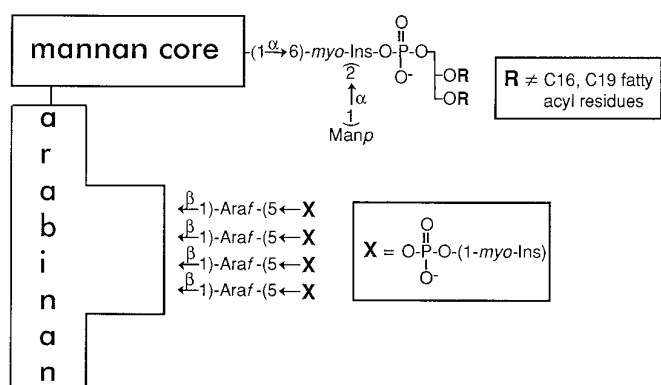


FIG. 10. Partial structural model proposed for the *M. smegmatis* AraLAMs called PI-GAMs.

rial origin, the LAMs share the mannan core, the phosphatidyl-*myo*-Ins anchor, and the arabinan domain. Furthermore, according to the structures of the arabinan side chain extremity, the LAMs were subdivided into two types, AraLAMs and ManLAMs (4). The AraLAMs, characterized by β -D-Araf caps (8), arise from an unidentified fast growing mycobacterial species, while the ManLAMs found in the slow growing species, *M. tuberculosis* (4, 5), *M. leprae* (8) and *M. bovis* BCG (6, 7) are typified by manno-oligosaccharides. However, the drawback of all the structural and biological LAMs studies is the fact that LAMs are not a single molecular species, as illustrated by the broad band observed in SDS-polyacrylamide gel electrophoresis (35) and more recently by matrix-assisted laser desorption-MS (3) studies showing precisely a 6-kDa molecular mass heterogeneity.

Nevertheless, it is now clearly established that all LAM activities, whatever their structure, require the alkali-labile residues. Thus, findings concerning the structure of LAMs, in their native forms, emphasize the importance of the development of new analytical approaches. Using two-dimensional ^1H - ^{13}C and ^1H - ^{31}P NMR experiments, we established that the LAMs from *M. smegmatis*, a fast growing mycobacterial strain, belong to the AraLAM class, but more interestingly the presence, the structure, and the location of mild alkali-labile and -stable phosphoinositides were unambiguously demonstrated.

First, the fact that the *M. smegmatis* LAM belongs to the AraLAM class was established by one-dimensional ^{13}C NMR and two-dimensional ^1H - ^{13}C HMQC experiments. From the t - α -D-Manp and the 2-*O*-linked α -D-Manp anomeric carbon resonances, it was found that each of them correlated with only one anomeric proton signal instead of two in the case of the ManLAMs from *M. bovis* BCG (6). Thus, the *M. smegmatis* LAMs are composed of *t*-Manp and 2,6-di-*O*-linked Manp units restricted to the mannan core, proving that they belong to the AraLAM class. During the preparation of this paper, similar data appeared in the literature using a different analytical approach based on the FAB-MS study of LAM acetolysates (8). However, this strategy, compared with NMR analysis, requires LAM chemical degradation followed by chromatography fractionation prior to FAB-MS analysis.

Second, unexpected structural features of mild alkali-labile and alkali-stable phosphoinositides were deduced, for the first time, by direct NMR studies of the native AraLAMs. The AraLAM one-dimensional ^{31}P spectrum unambiguously reveals the presence of two types of phosphodiester groups that resonate independently at -0.11 ppm (P1) and -0.35 ppm (P2) with an integration ratio of 1:4. Upon AraLAM treatment under mild alkaline conditions, P1 and P2 resonances are still present in the one-dimensional ^{31}P spectrum, but their relative intensities become similar, proving the presence of three mild

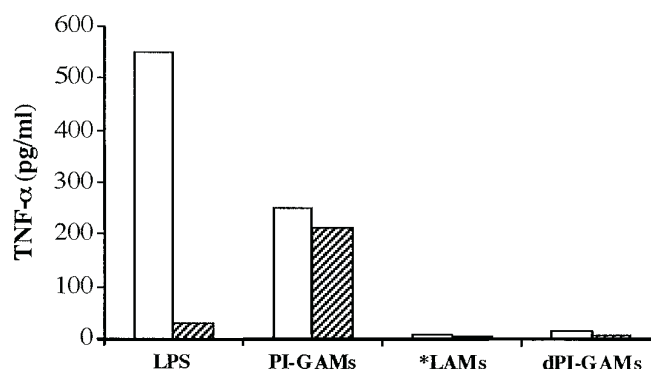


FIG. 11. TNF- α production by human monocyte/macrophage cell line THP-1 stimulated by LPS, PI-GAMs, deacylated PI-GAMs (*dPI*-GAMs), or LAMs (the *M. smegmatis* LAMs fraction analyzed was devoid of PI-GAMs) at $10 \mu\text{g/ml}$, preincubated in the presence (hatched bars) or absence (empty bars) of polymyxin B ($10 \mu\text{g/ml}$).

alkali-labile and two mild alkali-stable phosphodiester groups per molecule (Fig. 10).

The structures of the P1 and P2 substituents were directly determined from the native and the mild alkaline-treated AraLAMs by two-dimensional ^1H - ^{31}P HMQC-HOHAHA experiments. Starting from the alkali-stable P1 resonance at $\delta -0.11$, a diester linkage with Gro and *myo*-Ins was established, typifying a part of the well-known phosphatidyl-*myo*-Ins anchor. Likewise, starting from the alkali-stable P2 resonance at -0.35 ppm, the ^1H - ^{31}P HMQC-HOHAHA spectra support a phosphodiester linkage between a monosaccharide assigned to β -D-Araf (correlation with an anomeric proton, $J_{1,2} = 3.15$ Hz) and *myo*-Ins. This NMR approach applied to the native AraLAM P2 resonance at -0.35 ppm reveals the same substituent structure (*myo*-Ins)-P2-(β -D-Araf) for the mild alkali-labile and mild alkali-stable P2. The terminal location of the four P2-*myo*-Ins units was unambiguously determined from their ^1H chemical shifts. Moreover, the ^1H - ^{31}P HMQC experiments from the alkali-stable and -labile P2 show the same pattern characterized by three connectivities, one with the H-1 of the *t*-*myo*-Ins and the two others with the prochiral H-5 and H-5' of the β -D-Araf, revealing that P2 binds the β -D-Araf at C-5 and the *t*-*myo*-Ins at C-1. On the basis of these NMR data, it was proposed that the *M. smegmatis* AraLAMs contain two mild alkali-stable phospho-*myo*-Ins, one assigned to the well known phosphatidyl-*myo*-Ins and the other to the unexpected (*t*-*myo*-Ins-1)-P-(5- β -D-Araf), and three alkali-labile units attributed to (*t*-*myo*-Ins-1)-P-(5- β -D-Araf). All four (*t*-*myo*-Ins-1)-P2-(5- β -D-Araf) units were found to cap the arabinan side chains in a process involving mild acidic AraLAM hydrolysis, P4 gel filtration, and oligosaccharide analysis by ^{31}P NMR spectroscopy and FAB-MS.

The different behavior of the four P2 motifs, having the same substituent structures, toward mild alkaline hydrolysis was explained in terms of accessibility precluded by the AraLAM conformation. It was assumed that the three P2 alkali-labile units are exposed at the molecule surface, while the P2 alkali-stable unit must be hidden in the core of the molecule. This assumption was borne out by the fact that the P2 alkali stability almost disappeared when the P2 units were contained by small oligosaccharides (*t*-*myo*-Ins-1)-P2-(5- β -D-Araf)-(α -D-Araf)_{*n*} (*n* = 0–4) arising from AraLAM mild acidic hydrolysis.

In conclusion, the structural study of the *M. smegmatis* AraLAMs reveals the presence of four (*t*-*myo*-Ins-1)-P-(5- β -D-Araf) units capping the arabinan chains, three of these units being alkali-labile. *Myo*-Ins-P-Araf motifs were also identified by Khoo *et al.* (8) using FAB-MS analysis of arabinose-contain-

ing oligosaccharides obtained either from LAM acetolysates or enzymatically from alkali-deacylated LAMs produced by an unidentified fast growing mycobacterial species. However, the structure of these motifs was incomplete (the anomeric configuration was not reported, and the sugar carbon involved in the linkage was only suggested). Moreover, on the basis of our study, it can be suggested that most of the (t-*myo*-Ins-1)-P-(5- β -D-Araf) caps were lost during the LAM deacylation prior to enzymatic degradation and also during the permethylation step used to determine the proportion of phospho-*myo*-Ins caps. Indeed, only a minor portion (around 20%) of the arabinan side chains were found to be capped by P-*myo*-Ins in the case of the unidentified fast growing mycobacterial species (8). The same approach applied to the *M. smegmatis* LAMs suggested the absence of such caps (8). Using the same permethylation strategy (Table I), it was found that the number of terminal β -D-Araf was equal to the number of 3,5-di-*O*-linked Arafs in agreement with the absence of t- β -D-Araf caps. Nevertheless, from Table I and from the molecular weight of the mannan core,² it can be advanced that 40–50% of the arabinan side chains are capped by P2-*myo*-Ins units.

In the present report, we demonstrate that three phosphoinositide motifs capping the arabinan side chains are alkali-labile groups. Moreover, from the chemical shifts of the glycerol protons and preliminary GC analysis, it was found that the AraLAMs arising from *M. smegmatis* cell wall solvent extraction were devoid of C-16 and C-19 fatty acids, and are therefore probably localized at the cell wall surface. This structural feature leads to two relevant conclusions: (i) the definition of a new class of related AraLAM molecules, namely PI-GAMs (for phosphoinositols-glyceroarabinomannans), which are present in the crude lipoglycan fraction obtained from *M. smegmatis* cell walls, and (ii) the crucial importance of the alkali-labile phosphoinositides that appear to be key structural motifs that support most of the specific immunological properties of the lipoglycans concerning the stimulation of the macrophage activation through CD14 (36), which is the major cell surface receptor for monocyte activation.

Thus, the biological activity of the PI-GAMs in eliciting TNF- α secretion in a human monocytic cell line was compared with that of the *M. smegmatis* LAMs devoid of PI-GAMs. It was clearly established that in the case of *M. smegmatis* strain, the AraLAM activity concerning the induction of TNF- α is mainly mediated by the PI-GAMs. Indeed, the AraLAM fraction devoid of PI-GAMs and characterized by the presence of C-16 and C-19 fatty acids (data not shown) was found inactive, suggesting that the fatty acid residues of the phosphatidyl *myo*-Ins are not involved in this process. As described previously for the AraLAMs (10), the ability of the PI-GAMs, treated in mild alkaline condition, to stimulate TNF- α production is drastically reduced, supporting the likelihood that alkaline groups play a major role. Our data reveal that the exposed phosphoinositides, which are alkali-labile, are of key importance and may determine the macrophage early gene response during its interaction with *M. smegmatis*. Thus, the ability of the PI-GAMs to

trigger TNF- α response in promoting a potent macrophage antimicrobial activity could be the major molecular cause of the macrophage success in killing *M. smegmatis* cells. Therefore, the PI-GAMs seem important determinants of mycobacterial avirulence.

Acknowledgment—We gratefully acknowledge J. D. Bounéry for GC and GC/MS technical assistance.

REFERENCES

- Brennan, P. J., Hunter, S. W., McNeil, M., Chatterjee, D., and Daffé, M. (1990) in *Microbial Determinants of Virulence and Host Response* (Ayoub, E. M., Cassell, G. H., Branche, W. C., Jr., and Henry, T. J., eds) pp. 55–75, American Society for Microbiology, Washington, D. C.
- Daniel, T. M. (1984) in *The Mycobacteria: A Sourcebook* (Kubica, G. P., and Wayne, L. G., eds) pp. 417–465, Marcel Dekker Inc., New York
- Venisse, A., Rivière, M., Vercauteren, J., and Puzo, G. (1995) *J. Biol. Chem.* **270**, 15012–15021
- Chatterjee, D., Lowell, K., Rivoire, B., McNeil, M. R., and Brennan, P. J. (1992) *J. Biol. Chem.* **267**, 6234–6239
- Chatterjee, D., Khoo, K.-H., McNeil, M., Dell, A., Morris, H. R., and Brennan, P. J. (1993) *Glycobiology* **3**, 497–506
- Venisse, A., Berjeaud, J.-M., Chaurand, P., Gilleron, M., and Puzo, G. (1993) *J. Biol. Chem.* **268**, 12401–12411
- Prinzis, S., Chatterjee, D., and Brennan, P. J. (1993) *J. Gen. Microbiol.* **139**, 2649–2658
- Khoo, K.-H., Dell, A., Morris, H. R., Brennan, P. J., and Chatterjee, D. (1995) *J. Biol. Chem.* **270**, 12380–12389
- Chatterjee, D., Bozic, C. M., McNeil, M., and Brennan, P. J. (1991) *J. Biol. Chem.* **266**, 9652–9660
- Roach, T. I., Barton, C. H., Chatterjee, D., and Blackwell, J. M. (1993) *J. Immunol.* **150**, 1886–1896
- Roach, T. I., Chatterjee, D., and Blackwell, J. M. (1994) *Infect. Immun.* **62**, 1176–1184
- Zhang, Y., Doerfler, M., Lee, T. C., Guillemin, B., and Rom, W. N. (1993) *J. Clin. Invest.* **91**, 2076–2083
- Schlesinger, L. S. (1993) *J. Immunol.* **150**, 2920–2930
- Venisse, A., Fournié, J. J., and Puzo, G. (1995) *Eur. J. Biochem.* **231**, 440–447
- Sieling, P. A., Chatterjee, D., Porcelli, S. A., Prigozy, T. I., Mazzaccaro, R. J., Soriano, T., Bloom, B. R., Brenner, M. B., Kronenberg, M., Brennan, P. J., and Modlin, R. L. (1995) *Science* **269**, 227–230
- Barnes, P. F., Chatterjee, D., Abrams, J. S., Lu, S., Wang, E., Yamamura, M., Brennan, P. J., and Modlin, R. L. (1992) *J. Immunol.* **149**, 541–547
- Sibley, L. D., Hunter, S. W., Brennan, P. J., and Krahenbuhl, J. L. (1988) *Infect. Immun.* **56**, 1232–1236
- Hunter, S. W., and Brennan, P. J. (1990) *J. Biol. Chem.* **265**, 9272–9279
- Weber, P. L., and Gray, G. R. (1979) *Carbohydr. Res.* **74**, 259–278
- Ciucanu, I., and Kerek, F. (1984) *Carbohydr. Res.* **131**, 209–217
- Marion, D., and Wuthrich, K. (1983) *Biochem. Biophys. Res. Commun.* **113**, 967–974
- Bax, A., and Davis, D. G. (1985) *J. Magn. Res.* **65**, 355–360
- Bax, A., and Subramanian, S. (1986) *J. Magn. Res.* **67**, 565–569
- Shaka, A. J., Barker, P. B., and Freeman, R. (1985) *J. Magn. Reson.* **64**, 547–552
- Lerner, L., and Bax, A. (1986) *J. Magn. Res.* **69**, 375–380
- Adams, L. B., Fukutomi, Y., and Krahenbuhl, J. L. (1993) *Infect. Immun.* **61**, 4173–4181
- Espevik, T., and Nissen-Meyer, J. (1986) *J. Immunol. Methods* **95**, 99–105
- Henderson, T. O., Glonek, T., and Myers, T. C. (1974) *Biochemistry* **13**, 623–628
- Angyal, S. J., and Pickles, V. A. (1972) *Aust. J. Chem.* **25**, 1695–1710
- Angyal, S. J. (1979) *Carbohydr. Res.* **77**, 37–50
- Huang, Y., and Anderson, R. (1989) *J. Biol. Chem.* **264**, 18667–18672
- Glushka, J., Cassels, F. J., Carlson, R. W., and van Halbeek, H. (1992) *Biochemistry* **31**, 10741–10746
- Dahl, K. E., Shiratsuchi, H., Hamilton, B. D., Ellner, J. J., and Toossi, Z. (1996) *Infect. Immun.* **64**, 399–405
- Chatterjee, D., Roberts, A. D., Lowell, K., Brennan, P. J., and Orme, I. M. (1992) *Infect. Immun.* **60**, 1249–1253
- Hunter, S. W., Gaylord, H., and Brennan, P. J. (1986) *J. Biol. Chem.* **261**, 12345–12351
- Zhang, Y., Doerfler, M., Lee, T. C., Guillemin, B., and Rom, W. N. (1993) *J. Clin. Invest.* **91**, 2076–2083
- Cerdan, S., Hansen, C. A., Johanson, R., Inubushi, T., and Williamson, J. R. (1986) *J. Biol. Chem.* **261**, 14676–14680
- Johansson, C., Kordel, J., and Drakenberg, T. (1990) *Carbohydr. Res.* **207**, 177–183

² M. Gilleron, N. Himoudi, O. Adam, P. Constant, A. Venisse, M. Rivière, and G. Puzo, unpublished observation.